PHYSICAL REVIEW E VOLUME 47, NUMBER 3 MARCH 1993

Space-resolved x-ray emission from the densest part of laser plasmas: Molecular satellite features and asymmetrical wings

E. Leboucher-Dalimier, A. Poquérusse, and P. Angelo
Université Pierre et Marie Curie 75252 Paris CEDEX 05, France
and Laboratoire pour l'Utilisation des Lasers Intenses, Ecole Polytechnique, 91120 Palaiseau, France
(Received 30 July 1992)

We report on the analysis of space-resolved x-ray emission from the densest part of plasmas created by laser irradiation of plane targets. The plasmas are strongly correlated and not very emissive due to the high electron densities [$(1-3)\times10^{23}$ cm^{-3}] and the low temperatures (≤ 300 eV) involved. We present an alternative experimental technique that provides an extensive enhancement of the emission profiles. The Stark broadening of the F $L\beta$ and Al $L\beta$ lines is discussed with respect to asymmetries and the possible formation of transient molecules. Red satellites (molecular and dielectronic) on the low-energy wing of $L\beta$ are exhibited.

PACS number(s): 52.70.La, 52.25.Nr, 52.50.Jm, 32.70.−n

Technological advances in high-intensity lasers allow the generation of very strongly correlated plasmas. The present study concerns the x-ray emission from the ablation region of plane targets where high densities in the range $(1-3)\times10^{23}$ cm^{-3} and low electronic temperature (≤ 300 eV) are inferred. Although such plasmas can be easily produced with laser intensities higher than 2×10^{14} W cm^{-2}, there are several difficulties regarding the emission spectroscopic studies of Stark-broadened hydrogenlike and heliumlike lines. First, the emission coefficient is very low in the ultradense layer of the ablation region. Second, the emission from this region is difficult to access and to discriminate from the emission issuing from less dense regions. On the other hand, there are motivations to explore the ultradense region: the theoretical computation of line wings including multipolar effects leads to strong asymmetries [1–5]; in addition, several theoretical attempts indicate that strong ion collisions can form quasimolecules at very high densities [6–8].

In this paper, we describe an alternative experimental technique allowing access to dense plasma regimes hitherto unobtainable. By increasing the dense plasma volume selected by an angled spectrograph slit, the emission from this region becomes sufficient to explore the spectral line shapes using experimental results from only one laser shot. More precisely, we show that due to the high spatial discrimination with magnifications of 120, the measurements of spectral lines are significantly improved: the line wings are largely enhanced and show strong asymmetries and satellite features. These effects appear to be the experimental signature of the theoretical predictions discussed above. After a presentation of the new method, we report here, as a proof of its capability, the spatially resolved spectroscopic analysis of experiments concerned with Al, LiF, and CF_2 targets for which the $L\beta$ line shows asymmetrical wings at high densities. Fluorine has been chosen as an emitter candidate because of its large Stark effect. The F $L\beta$ line exhibits dielectronic satellites and unusual features at densities for which transient molecular structures could be involved. We show that, due to the high spatial resolution, a discrimination between the molecular satellite emission layer and the dielectronic satellite emission layer is possible. The dielectronic satellites' wavelengths have been calculated and we use a simple approach to give a possible explanation of the molecular features.

The experiments have been carried out by using the Nd-glass laser of the Laboratoire pour l'Utilisation des Lasers Intenses with wavelength $\lambda_L = 0.263$ μm and a pulse duration $\tau \approx 500$ ps. The observation of the above-mentioned effects (asymmetries and molecular features) needs a very high density $N_e \geq 10^{23}$ cm^{-3} and sufficient emission. Let us describe the experimental setup to access such dense regions. Numerical simulations for expanding plasmas show that such densities can be reached in the ablation region of plane targets for laser intensities greater than 2×10^{14} W cm^{-2}. These required intensities are consistent with the available 20–30-J energy shots onto focal spots of diameter $D = 200$ μm. This diameter has been experimentally determined so as to optimize the plasma emission: there are indeed two conflicting effects, namely the increase of the available emission volume with D and the subsequent laser intensity diminution with D^2, leading to the emission coefficient decrease. Two other means for enhancing high-density effects on the profiles have been developed here: (1) the target structure and implantation, and (2) the choice of the spatial integration domain.

First, regarding the targets, strips of aluminum, lithium fluoride (LiF), or polytetrafluorethylen (CF_2) are sandwiched between a silica or carbon substrate [Fig. 1(a)]. The targets are perpendicular to the laser beam (x direction) and well centered in the laser beam. The length of the plasma along the y axis is determined by the focal spot size D; the width l along the z axis is controlled by the fabrication of the targets. As l is smaller than D, the Al or F plasma is confined in a constrained flow by the substrate plasma. For all the experiments reported in this paper, l is also chosen smaller than 70 μm in order to control the radiative transfer in the z direction [9] or to take it off.

Next consider the spatial integration; the improvements in the implantation of the spectrograph PABURCE [10] are the following: The spatially resolving entrance slit is parallel to the x-y plane [Fig. 1(b)]. Its width (40 μm) ensures the spatial resolution (or integration) along the laser-target axis and its length parallel to the strip allows maximum emission. Moreover, the slit is

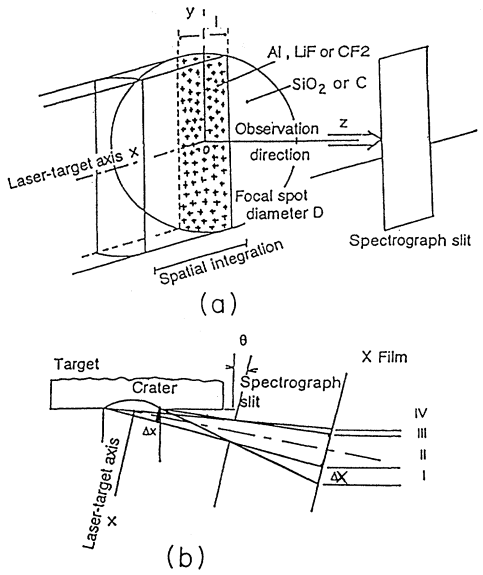

FIG. 1. (a) Geometry of the plasma issued from the plane target. (b) Spatial resolution of the spectrograph. The inclination angle θ with respect to the spectrograph axis allows a spatial integration over a large volume of dense plasma. Δx is the longest plasma path length through the dense plasma. $\Delta X = 120\Delta x$ on the film involves the dense part of the plasma.

angled so that the spectrograph axis has an inclination θ (8°–15°) with respect to the target plane. This new technique leads to an amplification of the maximum path length Δx [Fig. 1(b)] along the laser-target axis x, corresponding to the ultradense plasma. Consequently there appears a drastic enhancement of the ultradense effects in the line wings as detailed below. Locating the slit at 2 mm from the plasma leads to, first, an improvement on the signal-to-noise ratio and, second, a magnification ratio of 120 between a detected Δx plasma slab and the corresponding ΔX of the film. In Fig. 1(b) we can see that on the film there are four different regions corresponding to different spatial integrations in the plasma. Region I corresponds to a progressive integration over the whole of the densest part. For a target 40 μm wide and an inclination angle of 10°, the longest plasma path length through this ultradense part (the crater) is $\Delta x = 7$ μm, and the corresponding $\Delta X = 850$ μm on the film contains spectra involving plasma path lengths $\Delta x \leq 7$ μm. Progressively, in region II less dense plasma is involved and the contribution from the crater disappears in region III. In region IV the spatial integrations correspond to low-density plasma only.

We now discuss the line shapes observed on the films in the transverse direction. The high spectral resolution (2000) of the gradually bent concave KAP crystal allows the observation of very fine structures. The signals arising from those lines-of-sight that are integrals over the densest part of the plasma [i.e., region I, Fig. 1(b)] are shown in Fig. 2 for a 40-μm LiF target. The spectral range covering F $L\beta$ and its associated satellite transitions has been selected here. We know from previous results [11,12] that the density is greater than 5×10^{22} cm^{-3} because this density gave a rather good agreement between theoretical and experimental profiles of this line when emitted from the plasma region where its emission coefficient is maximum. Spectra (a)–(e) correspond to a varying dense plasma path length $\Delta x < 7$ μm. As Δx increases one progressively sees the enhancement of the line wings. On the spectra denoted (c) and (d) the line exhibits a very strong asymmetry and reveals two important satellites, referred to as (1) and (2) in the following. In Fig. 3 we show spectra involving dense and progressively less dense plasma [i.e., region II, Fig. 1(b)]. In the case of integrations over more than 7 μm along the laser-target axis, the satellites (1) and (2) disappear, whereas two other satellites denoted (3) and (4) appear very close to each other on (g) and (h). Moreover, we remark that for $\Delta x \geq 7$ μm the core of the main line is significantly enhanced while the wings remain with a steady intensity.

Concerning the satellites (3) and (4), they have been identified with He-like satellites of F $L\beta$. We used the analytical expressions given by Ivanov and Safronova [13] for these transitions stemming from doubly excited states. The formulas were obtained, averaged over quantum numbers LSJ, as functions of the number of electrons in the shells, taking into account relativistic effects. For the transitions $1s3s$-$3s3p$, $1s3p$-$3p^2$, and $1s3d$-$3p3d$, we found 12.753, 12.761, and 12.762 Å, respectively. These predictions are in good agreement with observation (see Fig. 3): the first satellite corresponds to our observed satellite (3), and the others, which are unresolved, correspond to satellite (4). As shown in Fig. 3 these dielectronic satellites are prominent only on the spectra involving more than 10 μm for the spatial integration along the laser-target axis. The emission volume includes lower densities $N_e < 5\times10^{22}$ cm^{-3} and higher temperatures $T_e > 200$ eV than in the crater; these conditions are propitious to dielectronic satellites. One can see that the $1s2s$-$2s3p$ and $1s2p$-$2p3p$ satellite positions that we have predicted approximately at 12.972 and 13.181 Å, are not

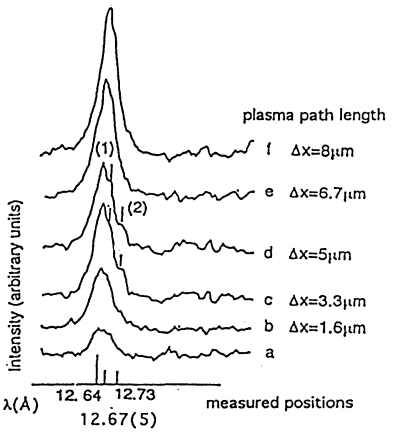

FIG. 2. F $L\beta$ space-integrated spectra. Target: $l = 40$ μm, $\theta = 10°$; laser beam: 16 J, 500 ps, 0.263 μm. Curves (a)–(f) correspond to varying dense plasma path length $\Delta x \leq 8\mu$m, as indicated in the figure. The spectra have been vertically shifted by arbitrary amounts. The red wing exhibits two satellites (1) and (2) in cases (c) and (d) only, corresponding to spatial integration over the largest ultradense volume. (1) and (2) are identified with molecular components of F $L\beta$, i.e., (101g)-(000u) and (220u)-(000g).

in the F $L\beta$ wavelength domain.

The features (1) and (2) (see Fig. 2) have been seen for the first time in the present experiments. Due to the technique developed in this paper, at every shot onto a thin target ($l \leq 50$ μm) the emission issued from the dense plasma and selected by the spectrograph was sufficient to show these prominent satellites in the enhanced asymmetrical wings. These features have been located at 0.03(5) Å and 0.09 Å from the main line. Since they are close to the resonance line, one should ask oneself whether they could be identified with dielectronic satellites involving an $n > 3$ spectator. There are at least two reasons for a negative answer: first, the population of a spectator $n > 3$ is less probable than that of a spectator $n = 3$, for given density and temperature, so that the intensity of such satellites should be smaller than the intensity of (3) and (4) in the region where they are emitted; secondly, the spatial discrimination between the satellites (3) and (4) on one hand and the features (1) and (2) on the other hand allowed us to put forward another proposal. We suggest that possible transient molecules in the target crater are responsible for the emission of the features (1) and (2). To support this conjecture, let us first recall a simple analysis that has been proven effective in neutral line-wing broadening. It is well known that in the ablation region of a plane target the Γ parameter measuring ion-ion coupling is larger than unity. Moreover, the average interionic spacing $R_i = [3(Z-k)/4\pi N_e]^{1/3}$ (N_e, electronic density; k, number of bound electrons) is comparable to the spatial extent of the excited-state orbitals, i.e., $n^2 a_0/Z$ (n, principal quantum number; a_0, Bohr radius). Thus the ion sphere model commonly used is not valid and the improvement in line broadening using a perturbative multipolar expansion [1–3] for the ionic microfield is not adequate either. The emitter cell considered must include bound electrons and two nearest-neighbor ionic centers. This molecular cell has to be embedded in a high-density free-electron plasma. A detailed calculation of the potential created by the plasma and its effects on the bound states of such an ionic molecule has been made [7,8] using self-consistent methods. These methods are suitable to ensure the coupling between the wave equation verified by the electronic bound states and the Poisson equation satisfied by the free electrons and the ionic centers. The Stark shift $\Delta\omega_{if}(R)$ for a transition $i \rightarrow f$ is defined by

$$\Delta\omega_{if}(R) \equiv \{[E_f(R) - E_i(R)]/\hbar\} - \omega_0 , \tag{1}$$

where $E_f(R)$ and $E_i(R)$ are the adiabatic energies of the transient molecule calculated within the Born-Oppenheimer approximation for i and f levels. R is the distance between the two ionic centers, and ω_0 is the unperturbed line frequency.

In the framework of the quasistatic limit of a nearest-neighbor theory, the line-wing shape is directly related to this shift and is given by

$$P(\omega) \propto \int \Pi(R) f_{if}(R) \delta\{\omega - [\omega_0 + \Delta\omega_{if}(R)]\} dR , \tag{2}$$

where $\Pi(R)$ stands for the nearest-neighbor probability and $f_{if}(R)$ for the transition oscillator strength. Writing

$$\delta\{\omega - [\omega_0 + \Delta\omega_{if}(R)]\} = \frac{\sum_\alpha \delta(R - R_\alpha(\omega))}{\left[\frac{\partial(E_f - E_i)}{\partial R}\right]_{R = R_\alpha(\omega)}} \hbar , \tag{3}$$

where the functions $R_\alpha(\omega)$ denote the roots of the implicit equation

$$\omega - [E_f(R) - E_i(R)]/\hbar = 0 , \tag{4}$$

one can see that singularities (i.e., molecular satellites) occur in the wings' profiles whenever the transition energy $E_f(R) - E_i(R)$ exhibits extrema with respect to R; we will denote by R_k these extrema and by ω_k the quantity $[E_f(R_k) - E_i(R_k)]/\hbar$.

In Ne X and F IX plasmas, for electronic densities $(1-3) \times 10^{23}$ cm^{-3} and electronic temperatures 200–300 eV, such extrema have been theoretically predicted [6,8] for two $L\beta$ components. We remark that these plasma parameters are consistent with the numerical estimates of the target crater parameters. We suggest that the experiments presented here are consistent with the formation of the molecule F^{8+}-F^{9+}. Numerical results [8] concerning this molecule have indeed shown that the adiabatic transition energies associated with two molecule components of F $L\beta$, i.e., $(101g) \rightarrow (000u)$ and $(200u) \rightarrow (000g)$ (notations with parabolic and azimuthal quantum numbers used for the separated atoms) reveal extrema. These extrema, computed for an electronic density $(1.2-1.5) \times 10^{23}$ cm^{-3} and an electronic temperature 230 eV, give singularities in pretty good agreement with the observed satellites (1) and (2) in the F $L\beta$ red wing.

In Fig. 4 we present another example where we have used the same experimental method to observe the emission from the densest part of an Al plasma. The spectra given cover the wavelength 6–6.2 Å with Al $L\beta$ and Si $L\alpha$ emissions. The latter occurs because a silica substrate was used. The Al $L\beta$ line was once again chosen because its line shape exhibits a strong Stark effect. The

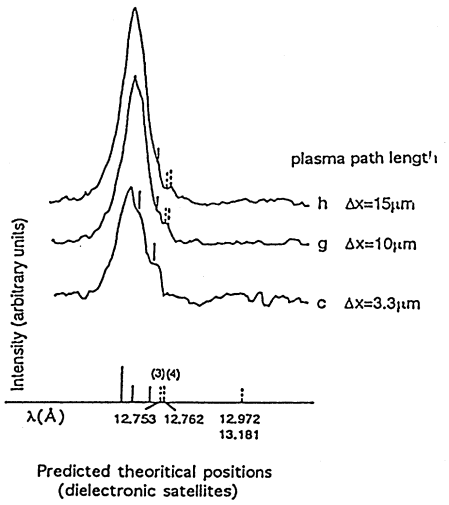

FIG. 3. Same as in Fig. 2 but for varying dense plasma path length $\Delta x \leq 15$ μm. Curves (g) and (h) involve less dense plasma. Satellites (1) and (2) disappear and the onset of two other satellites (3) and (4) can be seen. (3) and (4) are identified with He-like satellites of F $L\beta$, i.e., $1s3s$-$3s3p$, $1s3p$-$3p^2$, and $1s3d$-$3p3d$. The last two are unresolved.

spectra correspond to integrations over a wide range of emission volumes and one can distinguish between two kinds of spectra.

(i) The spectra with integrations over plasma path lengths along the laser-target axis $\Delta x < 20$ μm; i.e., those spectra that have contributions arising only from dense plasma (region I).

(ii) The spectra with integrations over $20 < \Delta x \leq 48$ μm, including emission from less dense plasma in addition to emission from the ultradense part (region II).

The limit of the two zones, 20 μm, is consistent with the dimension of the whole crater 75 sin(15°) μm projected along the laser-target axis. The region-I Al $L\beta$ spectra reveal a strong asymmetry with an important shoulder in the red wing. We attribute this bump to the presence of He-like dielectronic satellites $1s3s$-$3s3p$, $1s3p$-$3p^2$, and $1s3d$-$3p3d$ nearby. The computed positions (6.089, 6.091, and 6.091 Å, respectively) are in agreement with the observed spectra. For the region-II spectra, Al $L\beta$ wings are no longer enhanced and Al He-ε progressively appears as less dense plasma is involved.

In conclusion, we have shown that emission spectroscopy can be efficiently used to explore the densest part of a laser plasma originating from a plane target. Due to our experimental techniques, we obtain spectra with a great accuracy with regard to the intensity because of the selective enhancement of the emission and of the spatial resolution, and with regard to the wavelength because of the high spectral resolution. We remark that the time integration that induces a spatial smoothing over a plasma path length equivalent to the ablation depth was necessary for the enhancement of the emission. The investigation of these emitted spectral line shapes gives rise to several applications: first, it allows the analysis of particle (ions, electrons, molecules) correlations, which are of fundamental interest for equations of state; the line shapes also provide useful diagnostics of the ablation zone. Unusual asymmetries, molecular satellite and dielectric satellite features, have been exhibited. The satellites have been identified, and the spatial emission layers for these features have been accurately discriminated. We hypothesized the formation of the molecule F^{8+}-F^{9+} using a simple quasistatic approach for highly correlated fluorine plasmas. For a more precise study of the molecular satellites a complete generation of line broadening including dynamic effects will be necessary. With respect to its correlation parameter, the fluorine plasma considered here is similar to the high density core resulting from argon-filled microballoon implosions or to white dwarf stars. In these two cases satellite features have been seen: in microballoon implosions [14], the satellite seen in the blue wing of Ar He-α appears to have a molecular origin in the white dwarfs [15], the features in hydrogen $L\alpha$ have already been interpreted in terms of the formation of molecular structure (H-H^+ and H-H^+-H^+).

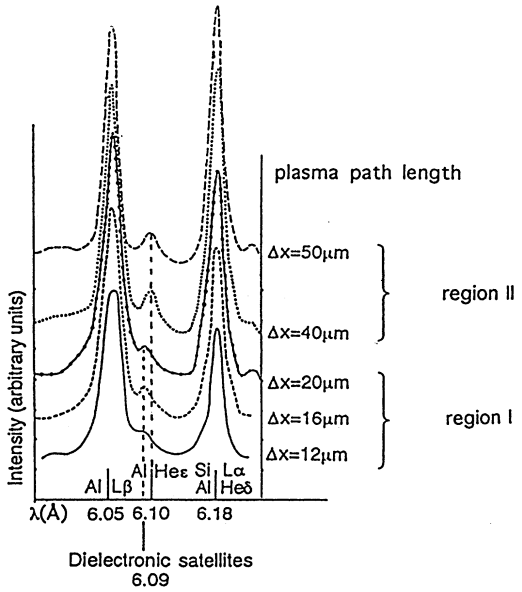

FIG. 4. Asymmetrical Al $L\beta$ and its He-like satellites. Target: $l = 75$ μm, $\theta = 15°$; laser beam: 23 J, 500 ps, 0.263 μm. The spectra involve integrations over $\Delta x \leq 20$ μm along the laser-target axis for region I and over $20 \leq \Delta x \leq$ %0 μm for region II. The spectra have been smoothed. When only the crater emission is involved (region I) He-like dielectronic satellites appear.

The authors acknowledge fruitful discussions with Ph. Malnoult and the expert technical assistance of M. Brisard. They thank C. Back of LLNL and D. Pesme of LULI for their helpful comments on this paper. They also want to thank P. Hammerling for his interest in our work. The Department de Recherches Physiques is "Unité de Recherche Associée au CNRS No. 0071." The Laboratoire pour l' Utilisation des Lasers Intenses is also affiliated with CNRS.

[1] A. V. Demura and G. V. Sholin, J. Quant. Spectrosc. Radiat. Transfer **15**, 881 (1975); A. V. Demura, in *Proceedings of the 11th ICSLS,* Carry le Rouet (France), 1992, edited by R. Stamm (Nova Science, New York, in press).

[2] L. Woltz and C. Hooper, in *Proceedings of the 2nd International Conference on Radiative Properties of Hot, Dense Matter,* edited by W. Goldstein (World Scientific, Singapore, 1987), p. 476.

[3] R. Joyce *et al.*, Phys. Rev. A **35**, 2228 (1987).

[4] D. Gilles (private communication).

[5] E. Leboucher *et al.*, in *Spectral Line Shapes 3,* edited by F. Rostas (de Gruyter, Berlin, 1985), p. 251.

[6] Ph. Malnoult *et al.*, Phys. Rev. A **40**, 1983 (1989).

[7] J. Stein *et al.*, Phys. Rev. A **39**, 2078 (1989); D. Salzmann *et al.*, *ibid.* **44**, 1270 (1991).

[8] Ph. Malnoult, thesis, Université de Paris (1989); and private communication.

[9] C. Bousquet *et al.*, J. Phys. B **23**, 1783 (1990).

[10] A. Poquérusse, Opt. Commun. **58**, 108 (1986).

[11] B. d'Etat *et al.*, J. Phys. B **20**, 1733 (1987).

[12] R. W. Lee, J. Quant. Spectrosc. Radiat. Transfer **40**, 561 (1988).

[13] I. A. Ivanov and U. I. Safronova, Opt. Spectrosk. **65**, 5 (1988) [Opt. Spectrosc. (USSR) **65**, 2 (1988)].

[14] C. F. Hooper, Jr. *et al.*, Phys. Rev. Lett. **63**, 267 (1989).

[15] J. Kielkopf, in *Proceedings of the 11th ICSLS* (Ref. [1]).